Manuscript submitted to: Volume 2, Issue 2, 61-78.

AIMS Materials Science DOI: 10.3934/matersci.2015.2.61

Received date 14 January 2015, Accepted date 07 April 2015, Published date 10 April 2015

Research article

Elastic Buckling Behaviour of General Multi-Layered Graphene Sheets

Rong Ming Lin

Aerospace Engineering Division, School of Mechanical and Aerospace Engineering, Nanyang Technological University, 639798 Singapore. E-mail: MRMLIN@NTU.EDU.SG; Tel: 65-679-04728.

Abstract: Elastic buckling behaviour of multi-layered graphene sheets is rigorously investigated. Van der Waals forces are modelled, to a first order approximation, as linear physical springs which connect the nodes between the layers. Critical buckling loads and their associated modes are established and analyzed under different boundary conditions, aspect ratios and compressive loading ratios in the case of graphene sheets compressed in two perpendicular directions. Various practically possible loading configurations are examined and their effect on buckling characteristics is assessed. To model more accurately the buckling behaviour of multi-layered graphene sheets, a physically more representative and realistic mixed boundary support concept is proposed and applied. For the fundamental buckling mode under mixed boundary support, the layers with different boundary supports deform similarly but non-identically, leading to resultant van der Waals bonding forces between the layers which in turn affect critical buckling load. Results are compared with existing known solutions to illustrate the excellent numerical accuracy of the proposed modelling approach. The buckling characteristics of graphene sheets presented in this paper form a comprehensive and wholesome study which can be used as potential structural design guideline when graphene sheets are employed for nano-scale sensing and actuation applications such as nano-electro-mechanical systems.

Keywords: buckling; critical loads; multi-layered graphene sheets; van der waals forces; differential quadrature

1. Introduction

Graphene is chemically one of the two allotropes of carbon in its spatial presentations in which a flat monolayer of carbon atoms are tightly packed into a two-dimensional honeycomb lattice [1]. It is the thinnest known film in the universe and the strongest ever measured in mechanical strength; its charge carriers exhibit extremely high intrinsic mobility and it can sustain current densities six orders of magnitude higher than that of copper; it has excellent thermal conductivity and superb optical performance. Fascinated by these newly discovered extraordinary and superb physical, mechanical, electrical, thermal and optical properties of graphene sheets, enormous research resources and efforts

have recently been directed to explore their fundamental properties and their potential engineering applications since they were first discovered in 2004 by Novoselov et al [2]. Studies of graphene sheets have since become a key fundamental issue in nanotechnology since fullerenes and carbon nanotubes can be generally considered as deformed graphite sheets. Among the many emerging and important applications, graphene has been notably employed as mechanical resonators [3–8] and physical sensors [9–12]. Nevertheless, successful applications of graphene, both as resonators and sensors, have led to an important area of research which needs to be accomplished. That is to establish structural characteristics of graphene sheets accurately and reliably when they are integrated into a resonator or a sensor system. Since controlled experimental characterizations at nanosacle are still difficult to achieve to date, various analytical/numerical methods of predicting these properties have been rigorously pursued recently. These methods can be roughly classified as atomistic-based methods and continuum-based methods.

Atomistic-based methods such as the classical molecular dynamics simulation [13], tight-binding molecular dynamics [14] and density function theory [15] have been employed to study rigorously mechanical properties of carbon nanotubes and graphene sheets in static bending, dynamic vibration and buckling behaviour. However, these simulation methods remain formidably expensive in computational requirement, even with today's computational efficiency and speed. As a result, researchers in this area have been constantly searching for more efficient computational methods. Recently, researchers have increasingly turned their attentions to the much more familiar continuum structural mechanics models with the promise that these can be applicable to nanoscale structural components such as graphene sheets. Alongside with these thoughts, many continuum structural mechanics models have been proposed during the last decade. These include the beam modelling proposed by Govindjee and Sackman [16] and Yoon et al. [17], the cylindrical shell model proposed by Ru et al. [18] and the space truss model by Li and Chou [19]. On the other hand, detailed vibration analysis based on continuum mechanics as well as molecular mechanics has been carried out by Chowdhury et al. [20]. Based on non-local elasticity and higher order shear deformation theory, vibration modes of single graphene sheets were established [21]. When embedded on elastic foundation, dynamic properties of single layered graphene sheet were examined and the effect of elastic foundation assessed by Murmu and Pradhan [22].

With reference to structural buckling analyses of graphene sheets, much research effort has been paid to the studies of critical buckling loads and modes of graphenes subject to in-plane loadings and a number of useful methods have been developed. By employing an atomistic modeling approach, Sakhaee-Pour investigated elastic buckling behavior of defect-free single-layered graphene sheet (SLGS) and used the simulation results to develop predictive equations via a statistical nonlinear regression model [23]. Buckling analysis of bi-axially compressed single-layered graphene sheets was studied using nonlocal continuum mechanics, taking into account of nonlocal size effects [24]. Higher order shear deformation theory was reformulated using the nonlocal differential constitutive relations and applied to study buckling characteristics of nano-plates such as single-layered graphene sheets [25]. Buckling behaviour of single-layered graphene sheet embedded in an elastic medium was examined together with and without nonlocal elasticity and small-size effect [26]. Using first-principles theoretical analysis, Kumar et al. [27] established the in-plane buckling characteristics of a graphene layer, and demonstrated a weakly linear component in the dispersion of graphene's flexural acoustic mode, which is believed to be quadratic. Wilber [28] formulated a nonlinear continuum model of a graphene sheet supported by a flat rigid substrate and used the model to analyze its buckling behaviour. Taziev and Prinz [29] studied the elastic buckling behavior of a defect-free single-layered graphene sheet deposited on a strained InGaAs substrate. On the other hand, buckling

behavior of a nanoscale circular graphene under uniform radial compression was studied by Farajpour et al. [30], together with nonlocal small size effect. Samaei et al. [31] investigated the effect of length scale on buckling behaviour of a single-layered graphene sheet embedded in a Pasternak elastic medium using a nonlocal Mindlin plate theory. Ansari and Rouhi [32] developed explicit formula to study the bi-axial buckling of monolayered graphene sheets based upon continuum mechanics and small scale effect. More recently, an atomistic finite element model was developed to study the buckling and vibration characteristics of single-layered graphene sheets by Rouhi and Ansari [33].

From the review of those existing work, it becomes obvious that much research has been conducted to date on the buckling behaviour of graphene sheets. However, most of these reported research focused on the simpler case of a single layered graphene and while buckling characteristics of a single layered graphene are important, stacked multi-layered graphene sheets are being more increasingly employed in practice for innovative engineering applications. When multi-layered graphene sheets are considered, their structural behaviour become far more complex since they are essentially assembled structural systems with inter-layer van der Waals bonding forces. As a result, modelling of buckling behaviour of multi-layered graphene sheets becomes more challenging, demanding more sophisticated numerical technique and appropriate treatment of bonding forces and boundary constraints. In this paper, elastic buckling behaviour of multi-layered graphene sheets in the presence of van der Waals bonding forces has been systematically and successfully investigated using generalized differential quadrature (GDQ). Van der Waal forces are modelled, to a first order approximation, as linear physical springs which connect the nodes between the layers. Critical buckling loads and their associated modes are established and analyzed under different boundary conditions, aspect ratios and compressive loading ratios in the case of graphene sheets compressed in two perpendicular directions. Various practically possible loading configurations are examined and their effect on buckling characteristics is assessed. To model more accurately the buckling behaviour of multi-layered graphene sheets, a physically more representative and realistic mixed boundary support concept is proposed and applied. For the fundamental buckling mode under mixed boundary support, the layers with different boundary supports deform similarly but non-identically, leading to resultant van der Waals bonding forces between the layers which in turn affect the critical buckling load. Results are compared with existing known solutions to illustrate the excellent accuracy of the proposed modelling approach. The buckling characteristics of graphene sheets presented in this paper form a comprehensive and wholesome study which can be used as potential structural design guideline when graphene sheets are employed for nano-scale sensing and actuation applications such as nano-electro-mechanical systems (NEMS).

2. Materials and Method

2.1. Equations of Motion for Buckling of Multi-layered Graphenes

Consider in general a multi-layered graphene sheets (MLGS) that is supported with given boundary conditions. The chemical bonds are assumed to be formed between the layers which are the van der Waals forces. The MLGS is modelled as a stack of plates of length of each plate a, width b, thickness h, mass density ρ, and Young's modulus E, as shown in Figure 1.

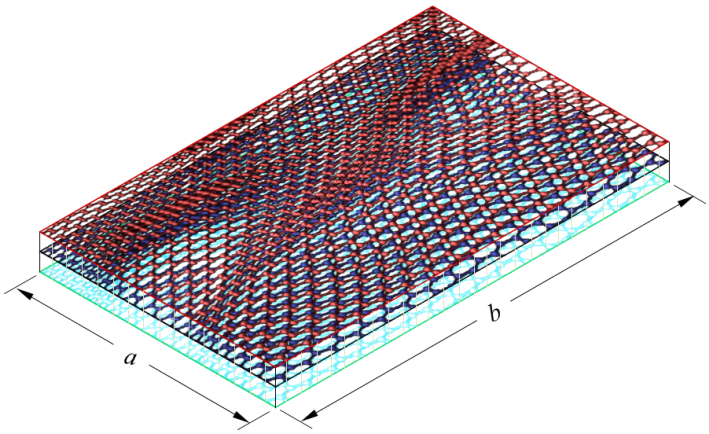

Figure 1. A multi-layered graphene sheets.

In the general case of L layered graphene sheets, each layer can be closely modelled as a plate with the chemical bonding forces between the layers to be modelled as pressure force applied to each of the layers, the L coupled equations of motion which govern the buckling characteristics of the graphene sheets can be written as,

$$\begin{cases} D\dfrac{\partial^4 w_1}{\partial x^4}+2D\dfrac{\partial^4 w_1}{\partial x^2\partial y^2}+D\dfrac{\partial^4 w_1}{\partial y^4}=q_1+\dfrac{N_x}{L}\dfrac{\partial^2 w_1}{\partial x^2}+\dfrac{N_y}{L}\dfrac{\partial^2 w_1}{\partial y^2}+\dfrac{2N_{xy}}{L}\dfrac{\partial^2 w_1}{\partial x\partial y} \\ D\dfrac{\partial^4 w_2}{\partial x^4}+2D\dfrac{\partial^4 w_2}{\partial x^2\partial y^2}+D\dfrac{\partial^4 w_2}{\partial y^4}=q_2+\dfrac{N_x}{L}\dfrac{\partial^2 w_2}{\partial x^2}+\dfrac{N_y}{L}\dfrac{\partial^2 w_2}{\partial y^2}+\dfrac{2N_{xy}}{L}\dfrac{\partial^2 w_2}{\partial x\partial y} \\ \vdots \\ D\dfrac{\partial^4 w_L}{\partial x^4}+2D\dfrac{\partial^4 w_L}{\partial x^2\partial y^2}+D\dfrac{\partial^4 w_L}{\partial y^4}=q_L+\dfrac{N_x}{L}\dfrac{\partial^2 w_L}{\partial x^2}+\dfrac{N_y}{L}\dfrac{\partial^2 w_L}{\partial y^2}+\dfrac{2N_{xy}}{L}\dfrac{\partial^2 w_L}{\partial x\partial y} \end{cases} \tag{1}$$

where x is the lengthwise and y is the breadthwise coordinates, w_i (i=1, 2, …, L) is the buckling displacement of ith graphene sheet, which is assumed to be positive upwards, D is the flexural rigidity of the individual sheet, q_i is the pressure that is exerted on sheet i due to the van der Waals interactions between the layers, and N_x, N_y, and N_{xy} are the uniform external forces in x and y directions and the shear force. The equilibrium distance between two neighbouring sheets is assumed to be 0.34 nm [34]. The initial pressure between layers in the absence of buckling deformation can be assumed to be negligible if the initial interlayer gap is taken as 0.34 nm. When buckling deformation is considered, the pressure can then be expressed as linearly proportional to the relative deflections between the layers,

$$q_i = \sum_{j=1}^{L} c_{ij}\left(w_i - w_j\right) \tag{2}$$

where the coefficients c_{ij} are derived in [35] by differentiating the potential function given in [34] ,

$$c_{ij} = -\left(\frac{4\sqrt{3}}{9a_{cc}}\right)^2 \frac{3\pi\varepsilon}{\sigma^2}\left(\frac{\sigma}{a_{cc}}\right)^8 \times \left[\frac{3003}{32}\sum_{k=0}^{5}\frac{(-1)^k}{2k+1}\binom{5}{k}\left(\frac{\sigma}{a_{cc}}\right)^6\left(\bar{z}_i-\bar{z}_j\right)^{-12} - 35\sum_{k=0}^{2}\frac{(-1)^k}{2k+1}\binom{2}{k}\left(\bar{z}_i-\bar{z}_j\right)^{-6}\right] \quad (3)$$

where a_{cc} is the *C-C* carbon bond length taken as a_{cc} = 1.42Å, $\bar{z}_i = z_i/a_{cc}$ is the normalized coordinate of the ith layer in the thickness direction with origin at the mid-plane of the graphene sheets, ε and σ are parameters associated with the physical properties of the material and are assumed to be ε = 2.968 meV, and σ = 3.407Å [36].

Boundary conditions need to be specified before the buckling problem formulated in (1) can be solved. In the case of clamped edges, these become,

$$\begin{cases} w_i = \dfrac{\partial w_i}{\partial x} = 0 \qquad when \qquad x = 0,\ a \\ w_i = \dfrac{\partial w_i}{\partial y} = 0 \qquad when \qquad y = 0,\ b \\ \qquad i = 1,\ 2,\ \cdots,\ L. \end{cases} \quad (4)$$

In the case of simply supported edges, these boundary conditions become,

$$\begin{cases} w_i = \dfrac{\partial^2 w_1}{\partial x^2} = 0 \qquad when \qquad x = 0,\ a \\ w_i = \dfrac{\partial^2 w_i}{\partial y^2} = 0 \qquad when \qquad y = 0,\ b \\ \qquad i = 1,\ 2,\ \cdots,\ L. \end{cases} \quad (5)$$

In the general case of multi-directional buckling of graphenes subject simultaneously to N_x and N_y in x and y directions and shear force N_{xy}, it is customary to assume that the ratios between these forces are known and remain constant during the buckling process. Let $N_y = \alpha N_x$ and $N_{xy} = \gamma N_x$, then (1) can be re-written as,

$$\begin{cases} D\dfrac{\partial^4 w_1}{\partial x^4} + 2D\dfrac{\partial^4 w_1}{\partial x^2 \partial y^2} + D\dfrac{\partial^4 w_1}{\partial y^4} = q_1 + \dfrac{N_x}{L}\left(\dfrac{\partial^2 w_1}{\partial x^2} + \alpha\dfrac{\partial^2 w_1}{\partial y^2} + 2\gamma\dfrac{\partial^2 w_1}{\partial x \partial y}\right) \\ D\dfrac{\partial^4 w_2}{\partial x^4} + 2D\dfrac{\partial^4 w_2}{\partial x^2 \partial y^2} + D\dfrac{\partial^4 w_2}{\partial y^4} = q_2 + \dfrac{N_x}{L}\left(\dfrac{\partial^2 w_2}{\partial x^2} + \alpha\dfrac{\partial^2 w_2}{\partial y^2} + 2\gamma\dfrac{\partial^2 w_2}{\partial x \partial y}\right) \\ \qquad \vdots \\ D\dfrac{\partial^4 w_L}{\partial x^4} + 2D\dfrac{\partial^4 w_L}{\partial x^2 \partial y^2} + D\dfrac{\partial^4 w_L}{\partial y^4} = q_L + \dfrac{N_x}{L}\left(\dfrac{\partial^2 w_L}{\partial x^2} + \alpha\dfrac{\partial^2 w_L}{\partial y^2} + 2\gamma\dfrac{\partial^2 w_L}{\partial x \partial y}\right) \end{cases} \quad (6)$$

The general buckling problem of multi-layered graphene sheets formulated as equation (6) can be solved for all the critical buckling loads and buckling modes of interest using Generalized Differential Quadrature (GDQ) subject to boundary conditions of (4) or (5) and van der Waals interaction forces as specified in (2). In the special uni-directional buckling, the loading ratios are assumed to be $\alpha = 0$ and $\gamma = 0$.

2.2. Generalized Differential Quadrature Method

Generalized differential quadrature (GDQ) method was developed by Shu and Richards [37] for computational fluid mechanics and has been successfully developed and applied to a wide range of structural and dynamics problems [38]. The basic underlying principle of GDQ is that the partial derivative of a function with respect to a spatial variable at a grid point can be expressed as a linear weighted sum of the function values at all grid points defined for the computational domain [39]. In the case of a graphene sheet, the computational domain is defined as $0 \le x \le a,\ 0 \le y \le b$. If this domain is meshed as $N \times M$ grid points, then, in GDQ, the partial derivative of the displacement w can in general be written as [39],

$$\begin{cases} \left.\dfrac{\partial^n w}{\partial x^n}\right|_{\substack{x=x_i \\ y=y_j}} = \displaystyle\sum_{k=1}^{N} C_{ik}^{(n)} w(x_k, y_j) = \sum_{k=1}^{N} C_{ik}^{(n)} w_{kj} \\ \left.\dfrac{\partial^n w}{\partial y^n}\right|_{\substack{x=x_i \\ y=y_j}} = \displaystyle\sum_{k=1}^{M} \overline{C}_{jk}^{(n)} w(x_i, y_k) = \sum_{k=1}^{N} C_{jk}^{(n)} w_{ik} \end{cases} \tag{7}$$

where the weighting coefficients $C_{ij}^{(m)}$ required can be computed in a simple recursive fashion as discussed in detail in [39],

$$C_{ij}^{(1)} = \frac{\xi(x_i)}{(x_i - x_j)\,\xi(x_j)} \qquad (i, j = 1, 2, \cdots, N;\ i \ne j) \tag{8}$$

where $\xi(x_k)$ is defined as,

$$\xi(x_k) = \prod_{j=1;\ j \ne k}^{N} (x_k - x_j) \tag{9}$$

The special case when $i = j$, the $C_{ii}^{(1)}$ can be determined as,

$$C_{ii}^{(1)} = -\sum_{k=1,\,k \ne i}^{N} C_{ik}^{(1)} \qquad (i = 1, 2, \cdots, N) \tag{10}$$

Once the coefficients for first order derivatives are obtained, those for the second and higher order derivatives can be simply established based on following recurrence relationship,

$$C_{ij}^{(m)} = -\,m\left(C_{ii}^{(m-1)} C_{ij}^{(1)} - \frac{C_{ij}^{(m-1)}}{x_i - x_j}\right) \qquad (i, j = 1, 2, \cdots, N;\ i \ne j) \tag{11}$$

$$C_{ii}^{(m)} = -\sum_{k=1,\,k \ne i}^{N} C_{ik}^{(m-1)} \qquad (i = 1, 2, \cdots, N) \tag{12}$$

The corresponding coefficients $\bar{C}_{ij}^{(m)}$ associated with derivatives with respect to *y* required can be similarly determined [39].

In the case of buckling analysis, assuming transverse displacement of the *i*th layer as,

$$w_i(x,\ y) = W_i(X,\ Y) \qquad (i = 1,\ 2,\ \cdots,\ N) \tag{13}$$

where *X* and *Y* are the normalized non-dimensional coordinates used in numerical implementation. Upon substituting (13) into the general equation of motion (6), the following can be obtained in terms of unknown buckling displacement amplitude W_i and dimensionless critical buckling load parameter λ as,

$$\begin{cases} \dfrac{\partial^4 W_1}{\partial X^4} + 2\beta^2 \dfrac{\partial^4 W_1}{\partial X^2 \partial Y^2} + \beta^4 \dfrac{\partial^4 W_1}{\partial Y^4} = \displaystyle\sum_{k=1}^{L} \bar{c}_{1k} \left(W_1 - W_k\right) + \lambda \left(\dfrac{\partial^2 W_1}{\partial X^2} + 2\beta\gamma \dfrac{\partial^2 W_1}{\partial X \partial Y} + \beta^2 \alpha \dfrac{\partial^2 W_1}{\partial Y^2} \right) \\ \dfrac{\partial^4 W_2}{\partial X^4} + 2\beta^2 \dfrac{\partial^4 W_2}{\partial X^2 \partial Y^2} + \beta^4 \dfrac{\partial^4 W_2}{\partial Y^4} = \displaystyle\sum_{k=1}^{L} \bar{c}_{2k} \left(W_2 - W_k\right) + \lambda \left(\dfrac{\partial^2 W_2}{\partial X^2} + 2\beta\gamma \dfrac{\partial^2 W_2}{\partial X \partial Y} + \beta^2 \alpha \dfrac{\partial^2 W_2}{\partial Y^2} \right) \\ \qquad \vdots \\ \dfrac{\partial^4 W_L}{\partial X^4} + 2\beta^2 \dfrac{\partial^4 W_L}{\partial X^2 \partial Y^2} + \beta^4 \dfrac{\partial^4 W_L}{\partial Y^4} = \displaystyle\sum_{k=1}^{L} \bar{c}_{Lk} \left(W_L - W_k\right) + \lambda \left(\dfrac{\partial^2 W_L}{\partial X^2} + 2\beta\gamma \dfrac{\partial^2 W_L}{\partial X \partial Y} + \beta^2 \alpha \dfrac{\partial^2 W_L}{\partial Y^2} \right) \end{cases} \tag{14}$$

where $\beta = a/b$, $X = x/a$, $Y = y/b$, $\bar{c}_{ij} = c_{ij}a^4/D$, *a* and *b* are the length and width of the graphene sheet and the dimensionless critical load parameter λ is defined as,

$$\lambda = \frac{N_x a^2}{L D} \tag{15}$$

The above equation (14) can be discretized using GDQ as,

$$
\begin{cases}
\sum_{k=1}^{N} C_{ik}^{(4)}(W_1)_{kj} + 2\beta^2 \sum_{m=1}^{M} \overline{C}_{jm}^{(2)} \sum_{k=1}^{N} C_{ik}^{(2)} (W_1)_{km} + \beta^4 \sum_{m=1}^{M} \overline{C}_{jm}^{(4)} (W_1)_{im} = \\
\qquad \sum_{k=1}^{L} \overline{c}_{1k} \left[(W_1)_{ij} - (W_k)_{ij} \right] + \lambda \sum_{k=1}^{N} C_{ik}^{(2)} (W_1)_{kj} + 2\beta\gamma\lambda \sum_{m=1}^{M} \overline{C}_{jm}^{(1)} \sum_{k=1}^{N} C_{ik}^{(1)} (W_1)_{km} + \beta^2 \alpha\lambda \sum_{m=1}^{M} \overline{C}_{jm}^{(2)} (W_1)_{im} \\
\sum_{k=1}^{N} C_{ik}^{(4)}(W_2)_{kj} + 2\beta^2 \sum_{m=1}^{M} \overline{C}_{jm}^{(2)} \sum_{k=1}^{N} C_{ik}^{(2)} (W_2)_{km} + \beta^4 \sum_{m=1}^{M} \overline{C}_{jm}^{(4)} (W_2)_{im} = \\
\qquad \sum_{k=1}^{L} \overline{c}_{1k} \left[(W_2)_{ij} - (W_k)_{ij} \right] + \lambda \sum_{k=1}^{N} C_{ik}^{(2)} (W_2)_{kj} + 2\beta\gamma\lambda \sum_{m=1}^{M} \overline{C}_{jm}^{(1)} \sum_{k=1}^{N} C_{ik}^{(1)} (W_2)_{km} + \beta^2 \alpha\lambda \sum_{m=1}^{M} \overline{C}_{jm}^{(2)} (W_2)_{im} \\
\qquad \vdots \\
\sum_{k=1}^{N} C_{ik}^{(4)}(W_L)_{kj} + 2\beta^2 \sum_{m=1}^{M} \overline{C}_{jm}^{(2)} \sum_{k=1}^{N} C_{ik}^{(2)} (W_L)_{km} + \beta^4 \sum_{m=1}^{M} \overline{C}_{jm}^{(4)} (W_L)_{im} = \\
\qquad \sum_{k=1}^{L} \overline{c}_{1k} \left[(W_L)_{ij} - (W_k)_{ij} \right] + \lambda \sum_{k=1}^{N} C_{ik}^{(2)} (W_L)_{kj} + 2\beta\gamma\lambda \sum_{m=1}^{M} \overline{C}_{jm}^{(1)} \sum_{k=1}^{N} C_{ik}^{(1)} (W_L)_{km} + \beta^2 \alpha\lambda \sum_{m=1}^{M} \overline{C}_{jm}^{(2)} (W_L)_{im} \\
\qquad i = 1, 2, \cdots, N; \quad j = 1, 2, \cdots, M.
\end{cases}
\tag{16}
$$

Similarly, the boundary condition (4) can be discretized to become,

$$
\begin{cases}
(W_r)_{1j} = (W_r)_{Nj} = \sum_{k=1}^{N} C_{1k}^{(1)} (W_r)_{kj} = \sum_{k=1}^{N} C_{Nk}^{(1)} (W_r)_{kj} = 0 \\
(W_r)_{i1} = (W_r)_{iM} = \sum_{m=1}^{M} \overline{C}_{1k}^{(1)} (W_r)_{ik} = \sum_{m=1}^{M} \overline{C}_{Mm}^{(1)} (W_r)_{im} = 0 \\
r = 1, 2, \cdots, L; \quad i = 1, 2, \cdots, N; \quad j = 1, 2, \cdots, M
\end{cases}
\tag{17}
$$

Other boundary conditions can be similarly treated. In numerical implementation, (17) is solved for the displacements of the two lines of nodes next to the boundaries along all 4 edges which are expressed in terms of displacements of the remaining nodes. Such displacement relationships derived from boundary condition (17) are then incorporated in (16) to eliminate those displacements next to the boundaries, leading to a standard eigenvalue problem being formulated from which, all the critical buckling loads and buckling modes of the graphene sheets with given boundary conditions can be computed.

3. Results and Discussion

The main focus of this paper is on buckling analysis of MLGSs in which the layers are bonded through van der Waals interactions. But first, single layered grapheme sheets under various boundary and loading conditions are studied and results compared with known solutions available to fully establish the practical capability of the proposed aproach. For convenience of practical implementations, uniform grid point distributions are assumed throughout numerical simulations in

this paper although non-uniform grid distributions have been used and reported with good performance [39]. For a square graphene sheet, its length is assumed to be a = 10 μm, its thickness h = 0.34 nm, Young's modulus E = 1.06 TPa, Poisson's ratio ν = 0.25, and the mass density ρ = 2250 kg/m^3. The buckling modes with all edges simply supported are computed and are shown in Fig. 2 in the case of $N \times M = 25 \times 25$ corresponding to an eigenvalue problem of 441 active degrees of freedom. These modes are ordered according to the half wave number m, which gives the number of half waves into which the graphene buckles in the direction of compressive loading.

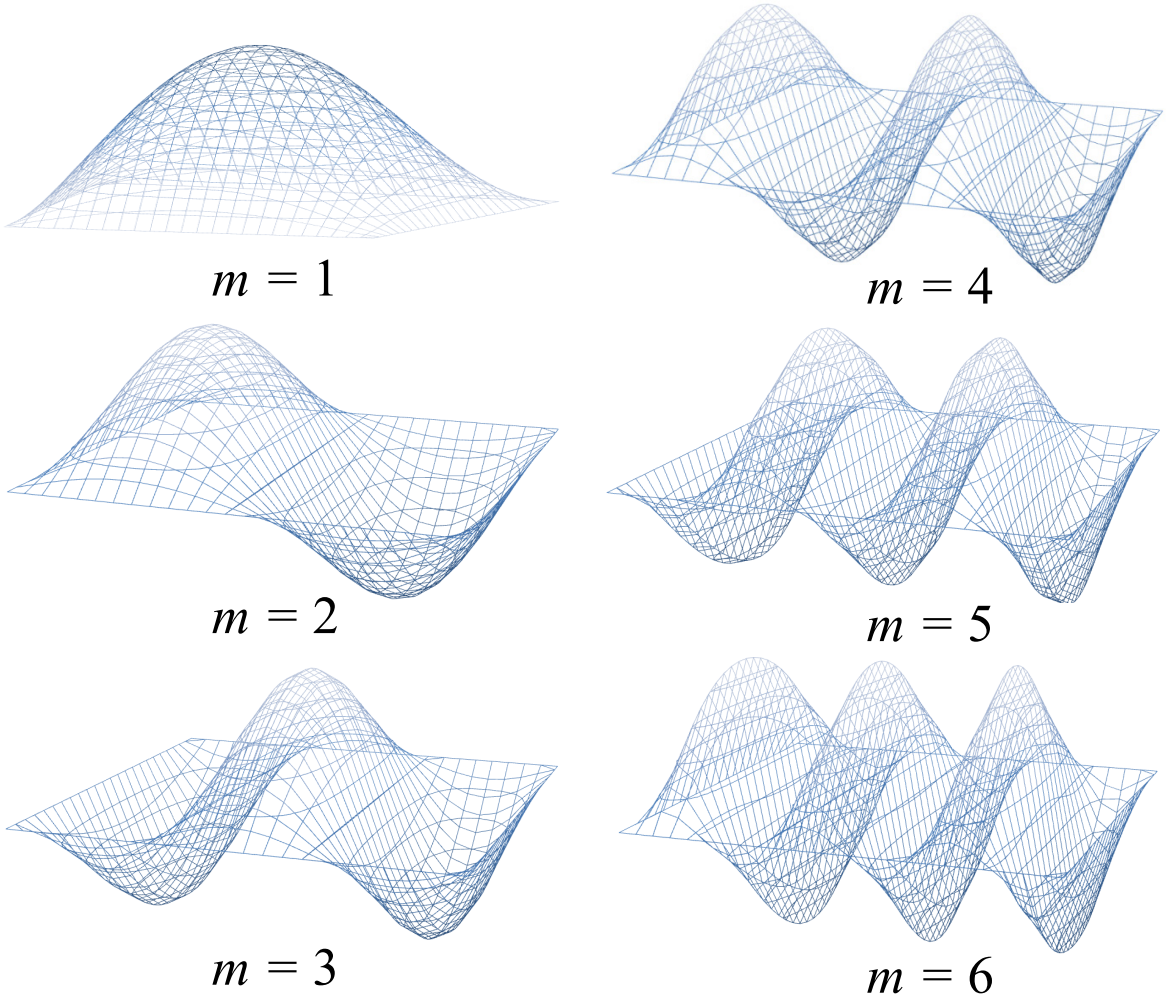

Figure 2. First 6 buckling modes of a simply supported square grapheme.

The critical buckling loads associated with these buckling modes are shown in Table 1. For the special case of a square graphene with simply supported edges, exact solutions happen to exist [40] and these are compared with those predicted using the proposed approach. As can be seen from Table 1, the difference between these 2 sets of results is indeed very small, indicating the excellent numerical accuracy of the proposed method. Also included in Table 1 are those critical buckling loads of a square graphene with clamped boundary supports. Clearly, these buckling loads are much higher than those of simply supported due to more rigid constraints clamped supports introduce. From the dimensionless critical load parameter λ, one can derive the physical buckling load N_x based on the definition of λ in equation (15).

Table 1. Critical buckling loads of simply supported and clamped square graphenes.

Buckling Mode No.	S-S-S-S Support				C-C-C-C Support	
	λ	Exact [40]	% Error	N_x (μN/m)	λ	N_x (μN/m)
1	**39.4797**	**39.4784**	**0.0033 %**	**1.4610**	**99.4031**	**3.6785**
2	61.6970	61.6850	0.0245 %	2.2819	114.598	8.4872
3	109.728	109.662	0.0602 %	4.0599	245.662	18.188
4	178.318	178.270	0.0269 %	6.6037	264.803	19.606
5	267.020	266.874	0.0547 %	9.8886	475.779	35.226
6	375.652	375.320	0.0879 %	13.912	501.926	37.162

In practical buckling analysis, it is usually the lowest fundamental critical load which actually determines structural buckling strength and hence in subsequent discussions, only the first critical load will be considered. In buckling of rectangular graphenes, it is of practical interest to examine how the fundamental critical load changes as aspect ratio β and compressive loading ratio α in the case of loadings applied in two perpendicular directions change. For a square graphene, when one side length a is fixed (a = 10 μm), the change of the other side b leads to a change in β ($\beta \equiv a/b$), which in turn leads to a change in the computed fundamental critical load λ_1 as shown in Figure 3. It is interesting to note that a minimum critical load is observed when the graphene is square. The critical load λ_1 increases as β increases for $\beta > 1$. For $\beta < 1$ however, it decreases as β increases. This is due to the fact that for every β value greater than 1, there is a corresponding β value less than 1 which makes the two graphenes similar in geometrical shape and hence the same dimensionless critical load λ_1.

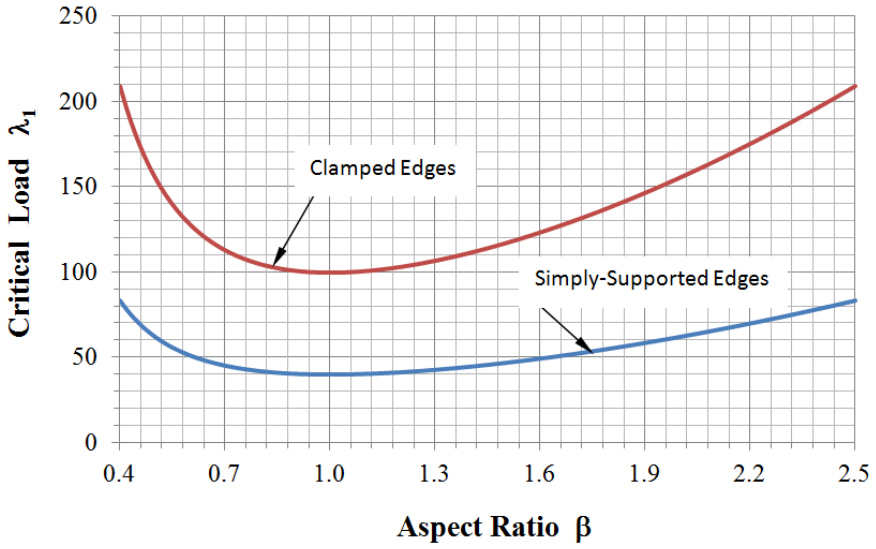

Figure 3. Critical load versus aspect ratio (a = 10 μm).

In the practical case where a graphene is simultaneously compressed in both x and y directions and the compressive loading ratio is known to be α, critical load in this case has been found to decrease considerably, especially for higher values of α. This means that under simultaneous x and y direction compressive forces, the magnitude of force required for a graphene to buckle becomes smaller than that of a single force applied in a one direction. This is illustrated clearly in Figure 4 in the case of a square graphene with side length a = 10 μm.

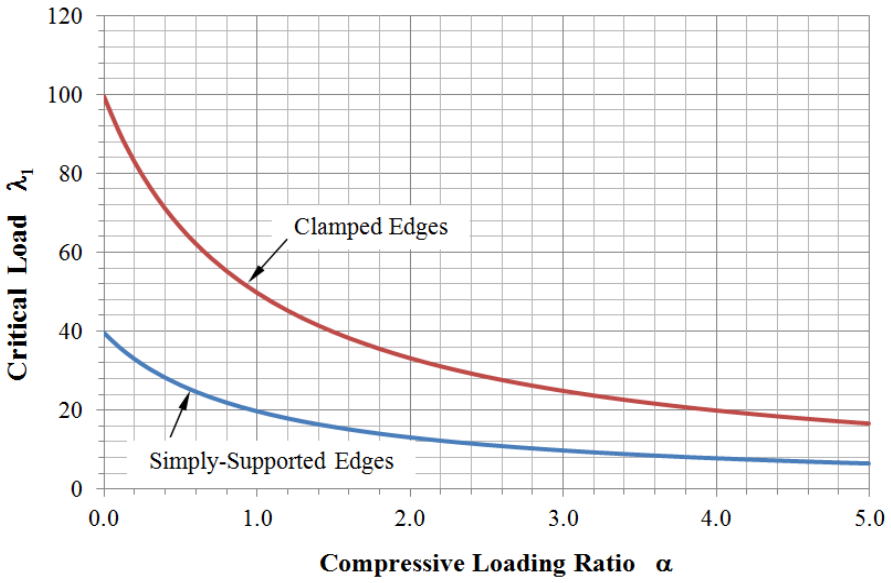

Figure 4. Critical load versus loading ratio of a square grapheme.

Similarly, when a graphene is subjected to two directional compressive loadings, for every given aspect ratio β value, the critical load required for the graphene to buckle becomes smaller than that required in the case of uni-directional loading. In the case of an assumed compressive loading ratio $\alpha = 1$, critical loads are computed at different values of β and these are shown in Figure 5. As compared with the results shown in Figure 2, the critical loads in this case of dual-directional loadings are about half of those obtained in the case of uni-directional loading when a compressive loading ratio $\alpha = 1$ is assumed.

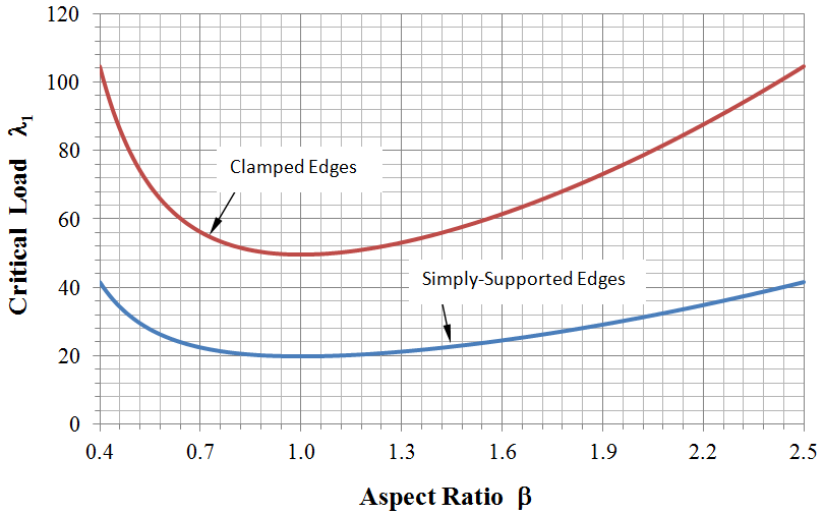

Figure 5. Critical load versus aspect ratio (a = 10 μm, $\alpha = 1$).

Graphenes are increasingly being deployed in many novel engineering applications such as NEMS in a multi-layered stacked form rather than a single layered isolated form, and as a result, accurate and reliable prediction of buckling behaviour of MLGSs becomes more important. One key difference in the modelling of buckling characteristics of MLGSs is the inclusion of van der Waals forces which hold the layers together as bonding forces. These forces are modelled, to a first order approximation, as linear springs which connect the layers and produce spring forces which are proportional to the relative displacements between the layers. Our analytical analysis and numerical simulations have demonstrated that for a MLGSs, when all the layers involved are assumed to be identical with assumed identical boundary supports, the layers will undergo the same displacement under buckling load as far as the fundamental mode is concerned. Such identical displacement pattern leads to no relative displacements between the layers and hence no additional van der Waals forces with reference to equilibrium state. The layers virtually deform independently of each other and as a result, the non-dimensional critical load λ_1 becomes the same as that of a single layer with the same boundary support. Nonetheless, the actual physical critical load N_x increases as the number of layer L increases as can be seen from equation (15) in which N_x is linearly proportional to L. So, having provided the buckling characteristics of single layered graphenes, buckling characteristics of MLGSs can be readily obtained if identical boundary supports for all the layers are assumed.

In practice however, such assumption of identical boundary supports is perhaps very unrealistic and erroneous since in any typical practical application of MLGSs, the surface layers and the internal layers are very likely to be subjected to different support conditions. A more accurate and physically more representative mixed boundary supports is desired to improve modelling accuracy. In view of the common physically clamped and substrate embedded edge supports of MLGSs in practice, it is perhaps more logical to model the surface layers as clamped support since for these layers, the rotations are constrained at the edges while the internal layers as simply-supported since they are almost free to rotate at the edges. Based on these practical observations and logical reasoning, a mixed boundary concept is proposed here and is applied to analyzed buckling characteristics of MLGSs. Critical load of MLGSs with as many as 30 layers has been computed using the proposed numerical approach and mixed boundary support concept, resulting in a non-symmetric eigenvalue problem of 265,230 active degrees of freedom. For a square 5-layered graphene sheets, its fundamental buckling mode is shown in Figure 6. The layers deform similarly as expected, but layers with different boundary supports have been found to have different values of displacement magnitudes, leading to van der Waals forces being generated which in turn affect the buckling of the graphenes.

It is interesting to note that as the number of layer increases, critical load decreases but it varies within the bounds provided by the case of all edges clamped and the case of all edges simply-supported, as shown in Figure 7. It is not difficult to see that as the layer increases, the overall effective support progressively approaches that of the case of all edges simply-supported and hence the critical load asymptotes its lower bound. These results vary considerably from those ideal cases of clamped and simply-supported for a typical given value of layer number L, demonstrating the practical significance and improved accuracy of the mixed boundary support approach.

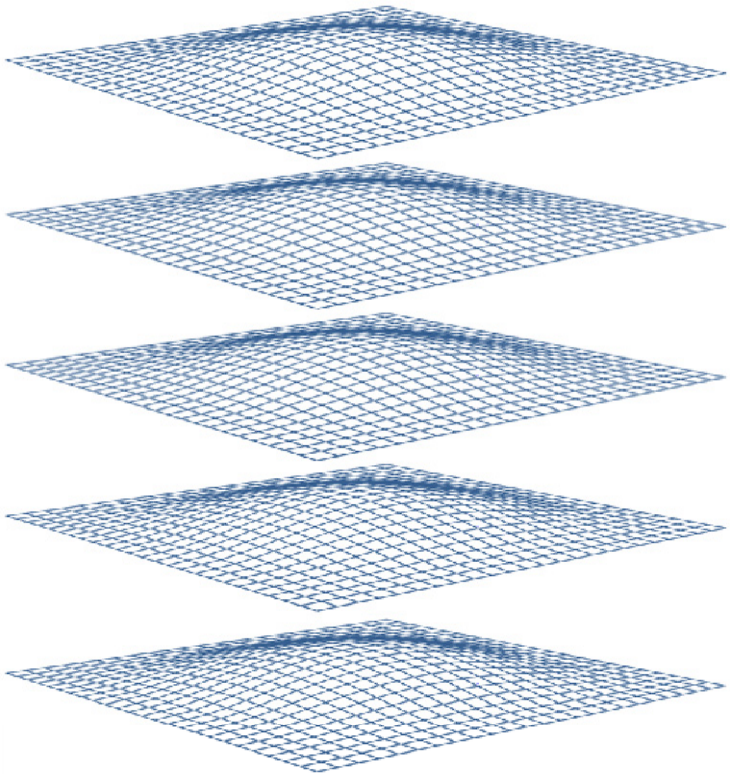

Figure 6. Fundamental buckling mode with mixed boundary supports.

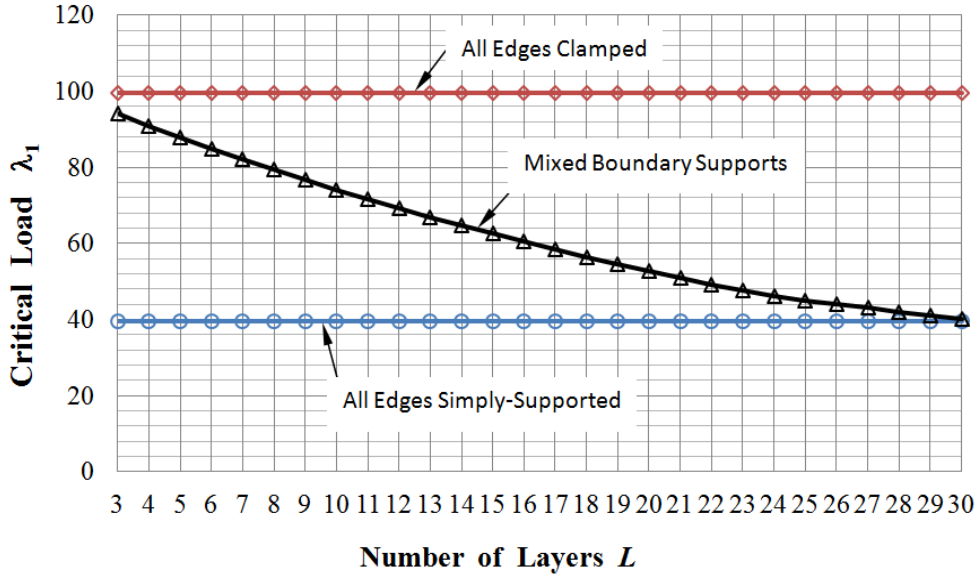

Figure 7. Critical loads of a square MLGSs with mixed boundary supports.

As expected, aspect ratios bear considerable effect on critical loads of MLGSs modelled with mixed boundary supports. These results are shown in Figure 8 in the case of uni-directional compressive loadings for a 5-layered and a 15-layered MLGSs. Similar to the case of a single layered graphene, a minimum critical load is found when $\beta = 1$ and increases with β for $\beta > 1$ and decreases with β for $\beta < 1$. However, the rates of increase or decrease become more moderate as compared with those of a single layer.

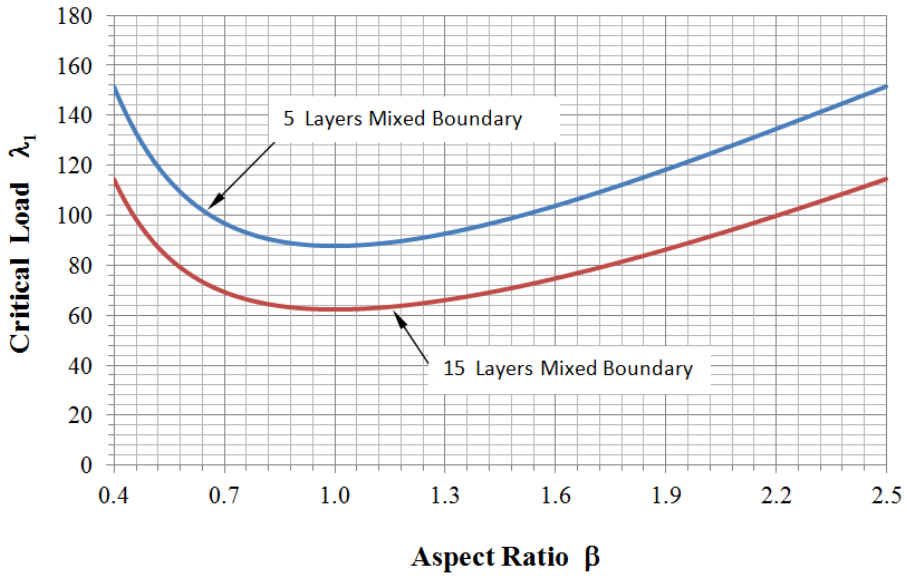

Figure 8. Critical load versus aspect ratio of MLGSs (a=10μm, α=0).

Another case of practical interest is the determination of critical buckling loads of MLGSs when subjected to dual directional compressive loadings. For a square MLGSs and a compressive loading ratio α = 1, critical loads are computed with different number of layers up to 30 and the results are shown in Figure 9, together with comparisons with those ideal cases of all edges clamped and all edges simply-supported. Again, critical loads are observed to be much lower as compared with those of uni-directional loadings.

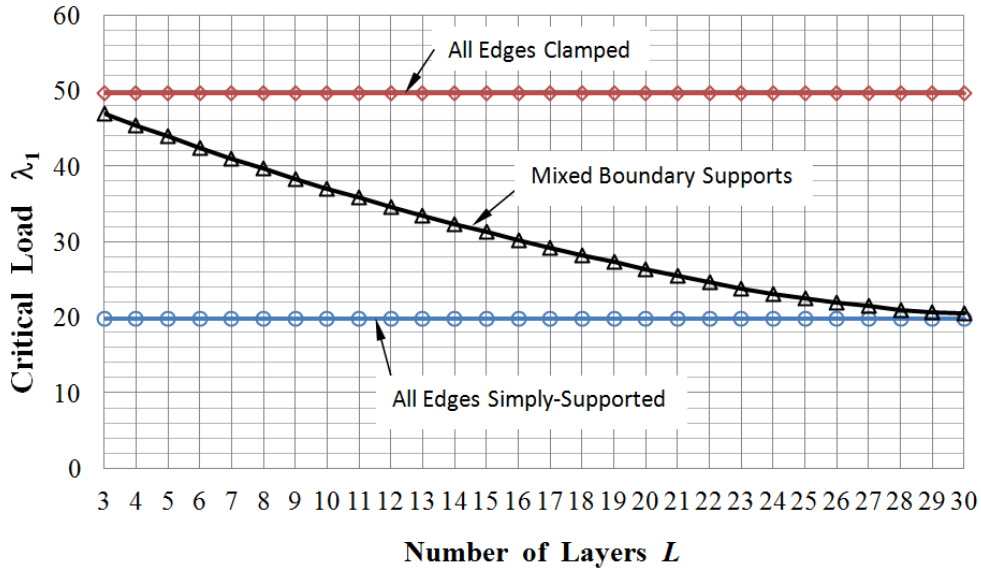

Figure 9. Critical loads of a square MLGSs under dual-directional load (α = 1).

In the case of dual-directional loadings, it is also important to establish how critical loads vary with aspect ratios when buckling characteristics of MLGSs are examined. These critical loads are computed for the case of compressive loading ratio α = 1 and are shown in Figure 10. Similar characteristics to those of Figure 7 are observed except that for the case of dual-directional loadings, critical loads become much lower as illustrated in Figure 10.

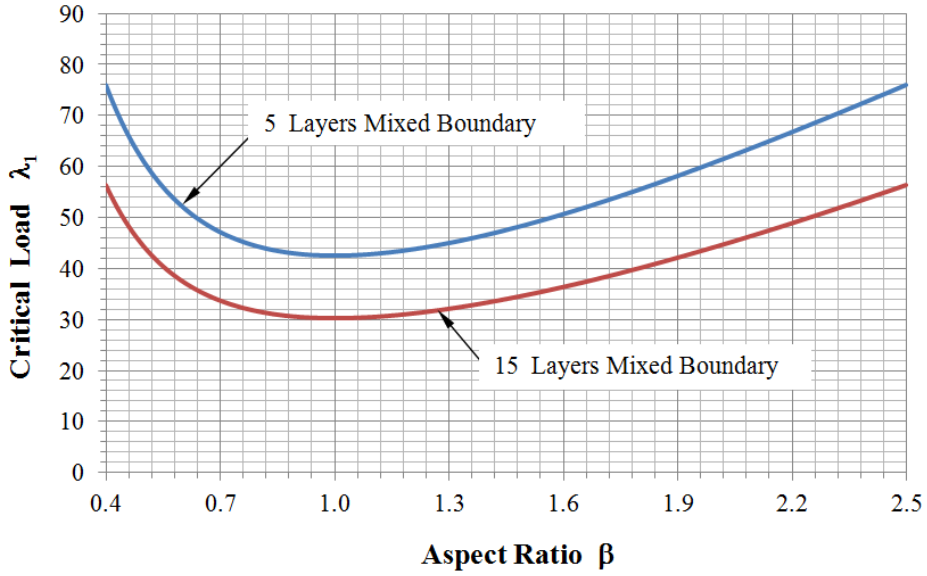

Figure 10. Critical load versus aspect ratio of MLGSs (a=10μm, α=1).

Based on the proposed numerical approach, the modelling of van der Waals interactions and the mixed boundary supports, extensive numerical simulations have been carried out to fully establish the buckling characteristics of single and multi-layered graphene sheets for various boundary conditions, aspect ratios, compressive loading ratios and number of layers. These results provide comprehensive and wholesome practically useful studies which can be used as potential structural design guideline when graphene sheets are deployed for various engineering applications where buckling strength becomes a major performance concern.

In practice however, nano-structured materials such as graphene sheets are often subjected to thermal loading due to temperature fluctuations in their applications, these thermal effect on buckling behaviour is not considered here in the present paper, though with the availability of thermal characteristics such thermal expansion coefficient, thermal loading effect can be accordingly treated [41]. In addition, as compared with those results obtained from atomic modelling of single layered graphene sheet [42], quite similar conclusions have been reached.

4. Conclusion

Multi-layered graphene sheets are increasingly being deployed for innovative sensing and actuation applications which often require detailed knowledge about their buckling strengths. However, structural modelling of MLGSs becomes more complex since they are essentially assembled structural systems with inter-layer van der Waals bonding forces. In this paper, elastic buckling behaviour of multi-layered graphene sheets in the presence of van der Waals bonding forces has been systematically and successfully investigated using generalized differential quadrature (GDQ). Van der Waal forces have been modelled, to a first order approximation, as linear physical springs which connect the nodes between the layers. Critical buckling loads and their associated modes have been established and analyzed under different boundary conditions, aspect ratios and compressive loading ratios in the case of graphene sheets compressed in two perpendicular directions. Various practically possible loading configurations have been examined and their effect on buckling characteristics has been assessed. To model more accurately the buckling behaviour of multi-layered graphene sheets, a physically more representative and realistic mixed boundary support concept has

been proposed and applied. For the fundamental buckling mode under mixed boundary support, the layers with different boundary supports deform similarly but non-identically, leading to resultant van der Waals bonding forces between the layers which in turn affect the critical buckling load. Results have been compared with existing known solutions to illustrate the excellent accuracy of the proposed modelling approach. The buckling characteristics of graphene sheets presented in this paper form a comprehensive and wholesome study which can be used as potential structural design guideline when graphene sheets are employed for nano-scale sensing and actuation applications such as nano-electro-mechanical systems (NEMS). The excellent accuracy and the general capability of the proposed approach have demonstrated its great potential for being used in general structural analysis of wide range of nano-structural systems.

References

1. Geim AK, Novoselov KS (2007) The rise of graphene. *Nature Mater* 6: 183–191.
2. Novoselov KS, Geim AK, Morozov SV, et al. (2004) Electric field effect in atomically thin carbon films. *Science* 306: 666–669.
3. Bunch JS, van der Zande1 AM, Verbridge SS, et al. (2007) Electromechanical resonators from graphene sheets. *Science* 315: 490–493.
4. Garcia-Sanchez D, van der Zande AM, Paulo AS, et al. (2008) Imaging mechanical vibration in suspended graphene sheets. *Nano Lett* 8: 1399–1403.
5. Chen C, Rosenblatt S, Bolotin KI, et al. (2009) Performance of monolayer graphene mechanical resonators with electrical readout. *Nature Nanotech* 4: 861–867.
6. van der Zande AM, Barton RA, Alden JS, et al. (2010) Large-scale arrays of single-layer graphene resonators. *Nano Lett* 10: 4869–4873.
7. Singh V, Sengupta S, Solanki1 HS, et al. (2010) Probing thermal expansion of graphene and modal dispersion at low-temperature using graphene nano-electro-mechanical systems resonators. *Nanotechnology* 21: 165204.
8. Song XF, Oksanen M, Sillanpää MA, et al. (2012) Stamp transferred suspended graphene mechanical resonator for radio frequency electrical readout. *Nano Lett* 12: 198–202.
9. Sakhaee-Pour A, Ahmadian MT, Vafai A (2008) Potential application of single-layered graphene sheet as strain sensor. *Solid State Commun* 147: 336–340.
10. Dan YP, Lu Y, Kybert NJ, et al. (2009) Intrinsic response of graphene vapour sensors. *Nano Lett* 9: 1472–1475.
11. Cheng ZG, Li Q, Li ZJ, et al. (2010) Suspended graphene sensors with improved signal and reduced noise. *Nano Lett* 10: 1864–1868.
12. Lu Y, Goldsmith BR, Kybert N, et al. (2010) DNA-decorated graphene chemical sensors. *Appl Phys Lett* 97: 083107.
13. Ijima S, Brabec C, Maiti A, et al. (1996) Structural flexibility of carbon nanotubes. *J Chem Phys* 104: 2089–2092.
14. Hernandez E, Goze C, Bernier P, et al. (1998) Elastic properties of C and $B_xC_yN_z$ composite nanotubes. *Phys Rev Lett* 80: 4502–4505.
15. Sanchez-Portal D, Artacho E, Soler JM, et al. (1999) Ab initio structural, elastic, and vibrational properties of carbon nanotubes. *Phys Rev B* 59: 12678–12688.
16. Govindjee S, Sackman JL (1999) On the use of continuum mechanics to estimate the properties of nanotubes *Solid State Commun* 110: 227–230.

17. Yoon J, Ru CQ, Mioduchowski A (2003) Vibration of an embedded multiwall carbon nanotube. *Composite Sci Technol* 63: 1533–1545.
18. Ru CQ (2000) Effective bending stiffness of carbon nanotubes. *Phys Rev B* 62: 9973–9976.
19. Li C, Chou TW (2003) A structural mechanics approach for the analysis of carbon nanotubes. *Int J Solids Structures* 40: 2487–2499.
20. Chowdhury R, Adhikari S, Scarpa F, et al. (2011) Transverse vibration of single-layer graphene sheets. *J Phys D—Appl Phys* 44: 205401
21. Pradhan SC, Sahu B (2010) Vibration of single layer graphene sheet based on non-local elasticity and higher order shear deformation theory. *J Comp Theor Nanosci* 7: 1042–1050.
22. Murmu T, Pradhan SC (2009) Vibration analysis of nano-single-layered graphene sheets embedded in elastic medium based on nonlocal elasticity theory. *J Appl Phys* 105: 064319.
23. Sakhaee-Pour A (2009) Elastic buckling of single-layered graphene sheet. *Comp Mater Sci* 45: 266–270.
24. Pradhan SC, Murmu T (2009) Small scale effect on the buckling of single-layered graphene sheets under biaxial compression via nonlocal continuum theory. *Comp Mater Sci* 47: 268–274.
25. Pradhan SC (2009) Buckling of single layer graphene sheet based on nonlocal elasticity and higher order shear deformation theory. *Phys Lett A* 373: 4182–4188.
26. Pradhan SC, Murmu T (2010) Small scale effect on the buckling analysis of single-layered graphene sheet embedded in an elastic medium based on nonlocal plate theory. *Physica E-Low Dimensional System Nanostructures* 42: 1293–1301.
27. Kumar S, Hembram KPSS, Waghmare UV (2010) Intrinsic buckling strength of graphene: First-principles density functional theory calculations. *Phys Rev B* 82: 11–15.
28. Wilber JP (2010) Buckling of Graphene Layers Supported by Rigid Substrates. *J Comp Theor Nanosci* 7: 2338–2348.
29. Taziev RM, Prinz VY (2011) Buckling of a single-layered graphene sheet on an initially strained InGaAs thin plate. *Nanotechnology* 22: 305705.
30. Farajpour A, Mohammadi M, Shahidi AR, et al. (2011) Axisymmetric buckling of the circular graphene sheets with the nonlocal continuum plate model. *Pysical E-Low-Dimensional Systems Nanotechnologies* 43: 1820–1825.
31. Samaei AT, Abbasion S, Mirsayar MM (2011) Buckling analysis of a single-layer graphene sheet embedded in an elastic medium based on nonlocal Mindlin plate theory. *Mech Res Commun* 38: 481–485.
32. Ansari R, Rouhi H (2012) Explicit analytical expressions for the critical buckling stresses in a monolayer graphene sheet based on nonlocal elasticity. *Solid State Commun* 152: 56–59.
33. Rouhi S, Ansari R (2012) Atomistic finite element model for axial buckling and vibration analysis of single-layered graphene sheets. *Physica E-Low-Dimensional Systems Nanostructures* 44: 764–772.
34. Girifalco LA, Lad RA (1956) Energy of Cohesion, Compressibility, and the Potential Energy Functions of the Graphite System. *J Chem Phys* 25: 693–697.
35. Jomehzadeh E, Saidi AR (2011) A study on large amplitude vibration of multilayered graphene sheets. *Comp Mater Sci* 50: 1043–1051.
36. Saito R, Matsuo R, T Kimura, et al. (2001) Anomalous potential barrier of double-wall carbon nanotube. *Chem Phys Lett* 348: 187–193.
37. Shu C, Richards BE (1992) Application of Generalized Differential Quadrature to Solve Two-Dimensional Imcompressible Navier-Stokes Equations. *Int J Numerical Methods Fluids* 15: 791–798.

38. Du H, Lim MK, Lin RM (1995) Application of Generalized Differential Quadrature to Vibration Analysis. *J Sound and Vibration* 181: 279–293.
39. Shu C (2000) Differential Quadrature and Its Application in Engineering, London, Springer-Verlag.
40. Timoshenko SP, Gere JM (1961) Theory of Elastic Stability, New York, McGraw-Hill.
41. Lin RM, Lim MK, Du H (1994) Large Deflection Analysis of Plates Under Thermal Loading. *Comp Method Appl Mech Eng* 117: 381–390.
42. Rouhi S, Ansari R (2012) Atomistic finite element model for axial buckling and vibration analysis of single-layered graphene sheets. *Physica E-Low-Dimensional Systems Nanostructures* 44: 764–772.